ACS OMEGA

Article

http://pubs.acs.org/journal/acsodf

Enhancing the Antibacterial Activity of Light-Activated Surfaces Containing Crystal Violet and ZnO Nanoparticles: Investigation of Nanoparticle Size, Capping Ligand, and Dopants

Sandeep K. Sehmi,[†,‡,§] Sacha Noimark,[∥] Sebastian D. Pike,[⊥] Joseph C. Bear,[‡] William J. Peveler,[‡] Charlotte K. Williams,[⊥] Milo S. P. Shaffer,[⊥] Elaine Allan,[§] Ivan P. Parkin,[‡] and Alexander J. MacRobert*[,†]

[†]UCL Division of Surgery and Interventional Science, University College London, Royal Free Campus, Rowland Hill Street, London NW3 2PF, U.K.

[‡]Materials Chemistry Research Centre, Department of Chemistry, University College London, 20 Gordon Street, London WC1H 0AJ, U.K.

[§]Division of Microbial Disease, UCL Eastman Dental Institute, University College London, 256 Gray's Inn Road, London WC1X 8LD, U.K.

[∥]Department of Medical Physics and Biomedical Engineering, University College London, Gower Street, London WC1E 6BT, U.K.

[⊥]Department of Chemistry, Imperial College London, Imperial College Road, London SW7 2AZ, U.K.

S *Supporting Information*

ABSTRACT: Healthcare-associated infections pose a serious risk for patients, staff, and visitors and are a severe burden on the National Health Service, costing at least £1 billion annually. Antimicrobial surfaces significantly contribute toward reducing the incidence of infections as they prevent bacterial adhesion and cause bacterial cell death. Using a simple, easily upscalable swell−encapsulation−shrink method, novel antimicrobial surfaces have been developed by incorporating metal oxide nanoparticles (NPs) and crystal violet (CV) dye into medical-grade polyurethane sheets. This study compares the bactericidal effects of polyurethane incorporating ZnO, Mg-doped ZnO, and MgO. All metal oxide NPs are well defined, with average diameters ranging from 2 to 18 nm. These materials demonstrate potent bactericidal activity when tested against clinically relevant bacteria such as *Escherichia coli* and *Staphylococcus aureus*. Additionally, these composites are tested against an epidemic strain of methicillin-resistant *Staphylococcus aureus* (MRSA) that is rife in hospitals throughout the UK. Furthermore, we have tested these materials using a low light intensity (∼500 lx), similar to that present in many clinical environments. The highest activity is achieved from polymer composites incorporating CV and ∼3 nm ZnO NPs, and the different performances of the metal oxides have been discussed.

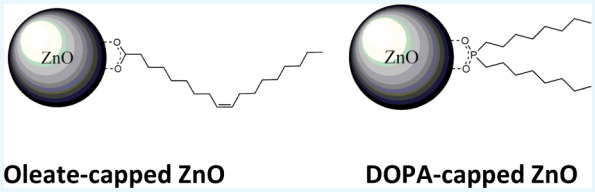

1. INTRODUCTION

Healthcare-associated infections (HCAIs) affect millions of patients worldwide, resulting in significant mortality and economic impact. This burden continues to grow as increasingly susceptible patients, such as the elderly or those suffering from chronic conditions, become more common.[1−3] It has been estimated that effective new antimicrobials used in combination with improved health/safety good practice could prevent an estimated 15−30% of HCAIs in the United Kingdom.[3,4] The development of such self-sterilizing surfaces in hospitals could sustainably reduce the HCAI rates over time by eliminating the transfer of bacteria that would usually occur from contact among patients, healthcare workers, and contaminated hospital surfaces.[5] One preventative strategy is to produce antimicrobial coatings that can kill the bacteria by continually delivering active compounds to the environment.[6] Such products include microbiocide-releasing surfaces and metal-coated surfaces (e.g., silver and copper).[5]

An alternative method for disinfecting surfaces is by coating them with light-activated antimicrobial agents, such as photosensitizers, which destroy bacteria via the production of reactive oxygen species (ROS) using photodynamic therapy (PDT).[7] Unlike other antimicrobials, radical species have nonspecific targets within a microbe, decreasing the likelihood of developing resistance.[8,9] Upon light activation, the photosensitizer molecules in their ground state are promoted to the lowest energy excited singlet state and can then undergo intersystem crossing to a longer-lived excited triplet state, which mediates the generation of cytotoxic ROS via type I or type II mechanistic pathways.[7] Type I involves the activated photosensitizer reacting directly with the substrate or molecule to form radicals, and type II involves the formation of singlet oxygen from ground-state molecular oxygen via the triplet

Received: April 19, 2016
Accepted: August 23, 2016
Published: September 6, 2016

DOI: 10.1021/acsomega.6b00017
ACS Omega 2016, 1, 334−343

state.[9] Common photosensitizers used to destroy cancerous tissues include Rose Bengal,[10,11] methylene blue,[8,12−16] and crystal violet (CV).[17−22] These photosensitizers can be coated onto polymers, and upon light activation, they generate ROS, causing oxidative damage and cell death.[21] We have previously reported a detailed description of the photochemical mechanisms involved in PDT.[20]

Dye-coated polymeric surfaces have shown significant enhancement of bactericidal activity when combined with various nanoparticles (NPs)[8,9,15,20−22] that display antibacterial properties relative to the bulk phase due to an increased surface area, leading to a greater particle surface reactivity.[23] ZnO NPs with antibacterial activity have received much interest for biomedical applications, as studies have shown them to have selective toxicity toward bacteria but minimal effects on mammalian cells.[20] The proposed mechanism of their antimicrobial activity is through photo-oxidative stress induced by ROS generation,[24] similar to the mechanism of photosensitizers. There have been various studies on the efficacious bactericidal effects of MgO,[25−29] and similar to ZnO, its advantages include affordability and biocompatibility. Properties such as size, morphology, concentration, and defects[30] can affect the antibacterial activity of NPs, for example, smaller sized NPs possess better antimicrobial action.[31]

It is well established in the literature that doping into ZnO host matrices can enhance their antibacterial activity by tuning their optical and electrical properties.[32−34] Zhang et al. reported that doping ZnO with Ag increased the antibacterial activity of ZnO,[30] and many studies have shown similar effects by doping ZnO with Sn,[35] Co,[33] and Mn.[34,36] Mg^{2+} ions are readily incorporated into the ZnO lattice by substitution due to the similar ionic radii of Mg^{2+} and Zn^{2+}.[37] It is reported that doping ZnO with Mg can change its electronic and luminescent properties, surface morphology, and defect density.[38] The surface (defect) structure is of particular interest with respect to the generation of ROS; therefore, investigating the effects of dopants on antibacterial activity is of interest.

In a previous study by our group, ∼18 nm ZnO NPs were synthesized via thermal decomposition of zinc oleate and encapsulated into medical-grade polyurethane squares that were coated with CV dye.[20] At a visible light intensity of ∼6600 lx, these samples were highly effective at reducing the numbers of *Escherichia coli* within 4 h and *Staphylococcus aureus* within only 1 h by ≥4 log. Such potent antibacterial activity was also observed against both the bacteria in the dark using the combination of CV and ZnO, demonstrating that a synergistic effect is responsible for the increased antibacterial activity shown by the dye and NP together.

In this article, we report the preparation of 15−18 nm sized Mg-doped ZnO (ZnMgO; 10% Mg) and MgO NPs capped with oleic acid (OA). These NPs are swell-encapsulated into CV-coated polyurethane, and their antibacterial activities are assessed in the dark and after exposure to visible light.[20] Alongside these larger NPs, we synthesized 2−4 nm sized di(octyl) phosphinic acid (DOPA)-capped ZnO and ZnMgO NPs (10% Mg), which were also incorporated with CV and encapsulated into polyurethane for antibacterial activity. For these samples incorporating smaller NPs, we used a much lower light intensity than that in the previous work (∼500 lx), as this is the level typically present in the clinical areas of a London teaching hospital (Prof. P. Wilson, personal communication). To further increase the relevance of our work to healthcare environments, we tested the bactericidal activity of our novel, biocompatible materials using an epidemic strain of methicillin-resistant *S. aureus* (EMRSA-16), one of two clones known to predominate in the United Kingdom (PHE). We hypothesized that the light-induced bactericidal activity of ZnO NPs in combination with CV will depend on the NP size and doping with Mg. Therefore, the primary aim of this study was to investigate whether the bactericidal activity of ZnO NPs is affected by the diameter, with and without Mg doping, using two different methods for preparing small doped ZnO NPs with diameters as small as 2 nm. We also examined the effect of the capping ligand on the antibacterial efficacy. Whereas we demonstrated that smaller ZnO NPs exhibit a higher bactericidal activity even without a photosensitizer, doping with Mg elicited no significant enhancement in the antibacterial activity of ZnO.

2. EXPERIMENTAL SECTION

2.1. Chemicals and Substrates. All chemicals and reagents described in the NP synthesis and material preparation were purchased from Sigma-Aldrich Chemical Co. except for toluene (Fischer Scientific, UK) and dichloromethane (DCM) (VWR, UK). Deionized water (resistivity 15 MΩ cm) was used in all synthetic work, and the substrate was medical-grade flat polyurethane sheets (thickness 0.8 mm) purchased from American Polyfilm Inc. (Branford, CT).

2.2. NP Synthesis. *2.2.1. OA-Capped NP Synthesis.* ZnMgO (10% Mg) and MgO NPs capped with OA were synthesized using a previously adapted method from Park et al.[39] Zinc(II) chloride (10 mmol, 1.36 g) and sodium oleate (20 mmol, 6.08 g) were added to a solvent mixture of ethanol, hexane, and deionized water (60 °C, 4 h) to produce zinc oleate. Sodium chloride was washed and removed, and the remaining organic layer was dried in vacuo to remove hexane, yielding zinc oleate as a white solid. Magnesium oleate was synthesized using the same procedure, with magnesium(II) chloride as the precursor. Zinc oleate (0.9 g), magnesium oleate (0.1 g), and OA (0.1784 mL) were dissolved in 1-octadecene (20 mL) and stirred at room temperature. The reaction mixture was heated to 320 °C under nitrogen (at a rate of 3.3 min^{-1}) and then held at 320 °C for 60 min. The resulting solution was allowed to cool, and the particles were precipitated with ethanol (80 mL). The solution was centrifuged, forming a solid precipitate (20 °C, 504*g*, 6 min), and the supernatant was discarded. The remaining solid precipitate was suspended in hexane (30 mL), producing a suspension of ZnMgO NPs. MgO NPs were synthesized via the same method by adding magnesium oleate (1.0 g) to OA and 1-octadecene and heating to 320 °C.

2.2.2. DOPA-Capped NP Synthesis. ZnO_DOPA NPs were synthesized as previously reported by Brown et al.[40] Briefly $ZnEt_2$ and 0.2 equiv of DOPA are dissolved in toluene, and to this a 0.4 M solution of water (in excess, 2 equiv used) in acetone is added dropwise to hydrolyze the organometallic reagent. Acetone is then added to precipitate the formed NPs, which are centrifuged, washed further with acetone, and left to air-dry overnight. To incorporate Mg, a mixture of $ZnEt_2$ and Mg(*sec*-Bu)(*n*-Bu) (0.7 M solution in hexane) was hydrolyzed with the ligand using the same synthetic protocol. A 9:1 ratio of Zn (300 mg, 2.43 mmol $ZnEt_2$) and Mg (268 mg 0.7 M solution, 0.27 mmol Mg(*sec*-Bu)(*n*-Bu)) reagents generated the desired 10% Mg doping level.

DOI: 10.1021/acsomega.6b00017
ACS Omega 2016, 1, 334−343

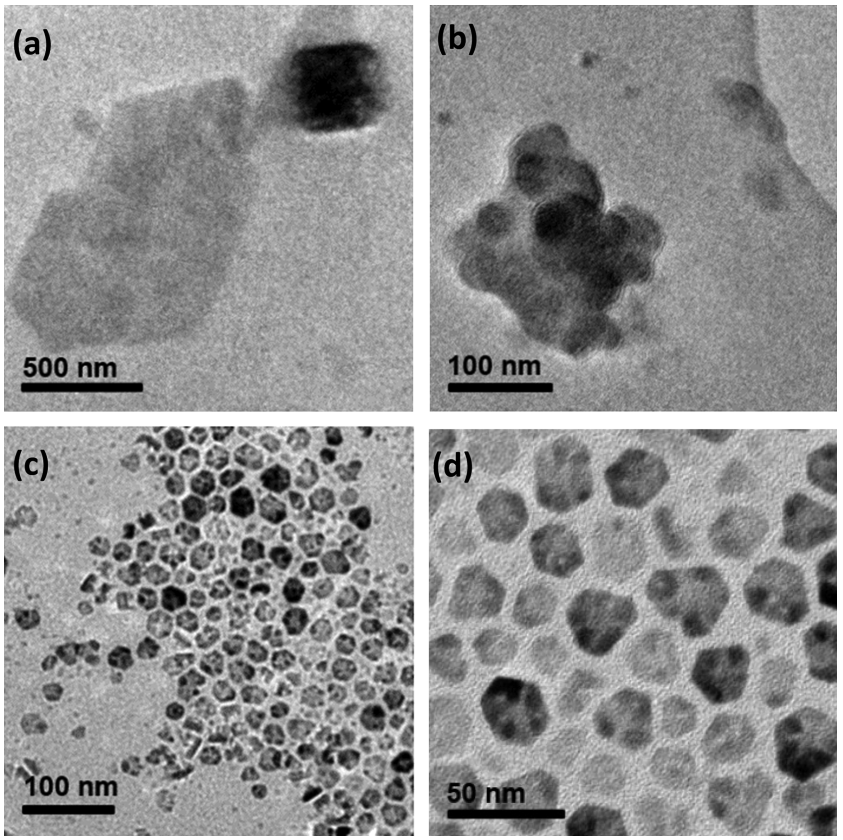

Figure 1. TEM images of (a, b) MgO NPs and (c, d) ZnMgO NPs.

3. METHODS

3.1. Material Preparation. Swelling solutions for incorporating NPs into polyurethane were prepared by immersing 1 cm^2 polymer squares into 1:1 hexane/DCM for OA-capped NPs and toluene for DOPA-capped NPs. A NP concentration of 1 mg/mL was used in both cases. The polymer samples were left to swell-encapsulate for 24 h and then dipped into 0.001 M aqueous solution of CV in water for 72 h (dark conditions). For the antibacterial investigation, control samples (only solvent treated) and polymer samples containing only NPs or CV were prepared.

3.2. Microbiology Assay. The following 1 cm^2 polyurethane samples were used: (1) solvent-treated sample (control), (2) NP-encapsulated polymer (MgO_OA, ZnMgO_OA, ZnMgO_DOPA, and ZnO_DOPA), (3) CV-coated polymer and (4) NP-encapsulated and CV-coated polymer (CVMgO_OA, CVZnMgO_OA, CVZnMgO_DOPA, and CVZnO_DOPA). The antibacterial activities of these samples were tested against those of *E. coli* ATCC 25922, *S. aureus* 8325-4,[41] and an epidemic strain of MRSA (EMRSA-16; *S. aureus* NCTC 13143), which is representative of one of the two types of methicillin-resistant *S. aureus* strains that dominate in UK hospitals.[42] These organisms were stored at −70 °C in Brain−Heart-Infusion broth (BHI; Oxoid) containing 20% (v/v) glycerol and propagated onto either MacConkey agar (Oxoid) in the case of *E. coli* or mannitol salt agar (Oxoid) in the case of MRSA for a maximum of two subcultures at intervals of 2 weeks.

The BHI broth was inoculated with one bacterial colony and cultured in air at 37 °C for 18 h, with shaking at 200 rpm. The bacterial pellet was recovered by centrifugation (20 °C, 2867.2*g*, 5 min), washed in phosphate-buffered saline (PBS) (10 mL), and centrifuged again to recover the pellet (20 °C, 2867.2*g*, 5 min), and the bacteria were finally resuspended in PBS (10 mL). The washed suspension was diluted 1000-fold to achieve an inoculum of ∼10^6 cfu/mL. In each experiment, the inoculum was confirmed by plating 10-fold serial dilutions on agar for viable counts. Triplicates of each polymer sample type were inoculated with 25 μL of the inoculum and covered with a sterile coverslip (2.2 cm^2). The samples were then irradiated for up to 6 h using either (a) a white-light source (General Electric 28 W Watt Miser compact fluorescent lamp) emitting an average light intensity of 6600 lx or (b) a white-light source used for general laboratory usage, emitting an average light intensity of 500 lx. A further set of samples was incubated in the dark for the same irradiation time.

After incubation, the inoculated samples and coverslips were added to PBS (450 μL) and mixed using a vortex mixer. The neat suspension and 10-fold serial dilutions were plated on agar for viable counts and incubated aerobically at 37 °C for 24 h (*E. coli*) or 48 h (*S. aureus*). The experiment was repeated three times, and the statistical significance of the following comparisons was analyzed using the Mann−Whitney *U* test: (1) control (polymer only) versus inoculum, (2) CV or NP versus control, (3) CV and NP versus CV alone.

4. RESULTS AND DISCUSSION

4.1. NP Synthesis and Characterization. Oleate-capped NPs were synthesized via a thermal decomposition method adapted from Park et al.[39] Metal oleate complexes were prepared by a salt metathesis reaction of a metal chloride and sodium oleate and heated up to 320 °C. Magnesium chloride was used instead of zinc chloride to synthesize magnesium

DOI: 10.1021/acsomega.6b00017
ACS Omega 2016, 1, 334−343

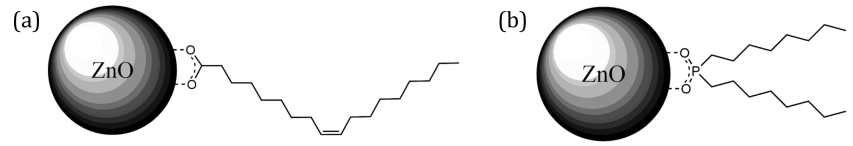

Figure 2. Diagram illustrating ZnO NPs capped with (a) OA and (b) DOPA.

oleate for MgO NPs, and a 9:1 ratio of zinc oleate and magnesium oleate was used to synthesize ZnMgO NPs. TEM images (Figures 1 and 2) and energy-dispersive X-ray (EDX) spectra were recorded, illustrating the discrepancies between the size and morphology of the NPs, despite having been synthesized using the same method. The MgO NPs were irregular in shape and formed clusters of up to 200−300 nm in diameter. TEM images of ZnMgO showed monodispersity, forming hexagonal truncated triangular plates (15 nm in average diameter size). The EDX spectra showed that the elemental composition of ZnMgO produced desired ratios well within the error limits, but the presence of magnesium in MgO NPs was difficult to detect (Figure S1, Supporting Information). XRD revealed a single phase for the doped ZnMgO NPs, corresponding to Wurtzite ZnO, suggesting that the Mg is intimately doped within the lattice, with no indication of a secondary phase (Figure S5). Analysis of the linewidths of the diffraction peaks using the Scherrer equation defined ZnMgO crystallites to have sizes of 5−10 nm, slightly smaller than those observed by TEM. It is possible that the larger particles observed by microscopy are made up of clusters of smaller crystallites.

On the basis of a Tauc plot (Figure S2), the band onset of oleate-capped ZnMgO NPs suspended in hexane was estimated to be 3.34 eV (similar to that of bulk ZnO, 3.3 eV), indicating that ZnMgO NPs are likely to act as UV-activated photocatalysts (<385 nm) and therefore should not exhibit significant white-light-activated bactericidal activity. As MgO NPs typically absorb at <159 nm, which is within the region that a solvent absorbs strongly in, it was not possible to determine the band gap of the oleate-capped MgO NPs suspended in hexane.

DOPA-capped NPs were synthesized by a method adapted by Brown et al.,[22,40] that is, by the controlled hydrolysis of $ZnEt_2$ in the presence of 0.2 equiv of DOPA. Likewise, DOPA-capped ZnMgO NPs were synthesized by hydrolyzing a 9:1 ratio of $ZnEt_2$ and $MgBu_2$ with the ligand. The sizes of the particles were determined from the XRD spectra (Figures S5−S7) using the Scherrer equation and gave estimated diameters of 2.2 (±0.3) and 2.8 (±0.2) nm for the ZnO and ZnMgO samples, respectively. The Mg-doped sample showed only one phase in the XRD spectrum, corresponding to Wurtzite ZnO; this gives us confidence that the Mg is well doped within the ZnO lattice. Inductively coupled plasma optical emission spectroscopy (ICP-OES) was used to confirm a 9:1 ratio of Zn/Mg in the doped sample. UV spectroscopy allows the determination of the band gap of these particles, with estimated band gaps of 3.7 (±0.1) and 3.6 (±0.1) eV, respectively (Figures S3 and S4).

4.2. Material Synthesis and Characterization. NPs were impregnated into medical-grade polyurethane (1 cm^2 squares).[19−22] Optimal incorporation of the NPs throughout the substrate was achieved by immersing the polymer squares in the NP swelling solutions for 24 h. A 1:1 ratio of hexane/DCM was used to encapsulate oleate-capped NPs, and toluene was used to swell-encapsulate DOPA-capped ZnO NPs into the polymer. The NP-incorporated polymers were subsequently dipped in a CV solution (0.001 M in distilled water, 72 h), resulting in polyurethane incorporating the following antimicrobial combinations:

(a) CV- and OA-capped metal oxide NPs: CVMgO_OA, CVZnMgO_OA, and CVZnO_OA.[1]
(b) CV- and DOPA-capped metal oxide NPs: CVZnMgO_DOPA and CVZnO_DOPA.

The modified polyurethane samples were analyzed using UV−vis absorbance spectroscopy. Because of the low concentration of NPs encapsulated in the polymer samples, no characteristic UV−vis absorption peaks in the visible region were observed. CV-coated polyurethane showed an absorbance maximum at λ = 590 nm, with a shoulder peak at λ = 548. The addition of NPs increased both the intensity and breadth of the CV peak for CVZnO_OA and CVZnO_DOPA samples. This trend continued for CVZnMgO_OA and CVZnMgO_DOPA, and for CVMgO_OA, the absorption reached its maximum. This was expected, as CVMgO_OA was darker in color than any other sample (Figure S8).

X-ray photoelectron spectroscopy (XPS) was used to determine whether the NPs were localized at the polymer surface or encapsulated throughout the bulk (Figure S9). XPS of CVZnMgO_OA did not show evidence of Mg (1s); however, a weak Mg peak was observed at 1304.0 eV for the CVMgO_OA sample. Notably, XPS has a detection limit of ∼0.1 atom %, indicating that MgO was present at a low concentration, correlating with the EDX data. XPS showed the presence of zinc on the surface of CVZnMgO_OA, with a doublet in the Zn (2p) region indicating Zn in ZnO. The XPS depth profile data demonstrated a decrease in zinc content within the polymer bulk. Peaks in the C (1s) region, N (1s) region, and O (1s) region were observed in the control and metal oxide NP-incorporated samples. A doublet in the Zn (2p) region was also indicated on the surface and within the polymer substrate for CVZnO_DOPA and CVZnMgO_DOPA. A peak in the Mg (1s) region was present for CVZnMgO_DOPA within the polymer substrate, but there was little indication of Mg (1s) present on the surface of the polymer.

Static equilibrium water contact measurements (∼5.0 μL) of all samples tested for antibacterial activity were recorded under standard laboratory conditions (Table S1). The results showed negligible differences between the hydrophobicities of the untreated and modified polyurethane samples (varying ±8° in contact angle). The photostability of CV, CVZnO_DOPA, and CVZnMgO_DOPA samples was examined with an ∼3880 lx white-light source for up to 60 days (Figure S10). UV−vis spectroscopy showed that CVZnO_DOPA and CVZnMgO_DOPA were photostable over a 60 day period, demonstrating 29 and 31% photodegradation, respectively, compared to that of CV (38%). This suggests that the materials are likely to exhibit long-term photostability under standard lighting within healthcare environments.

To encapsulate the NPs into polymers, certain solvents can be used to induce polymer swelling, such that NPs can diffuse

DOI: 10.1021/acsomega.6b00017
ACS Omega 2016, 1, 334−343

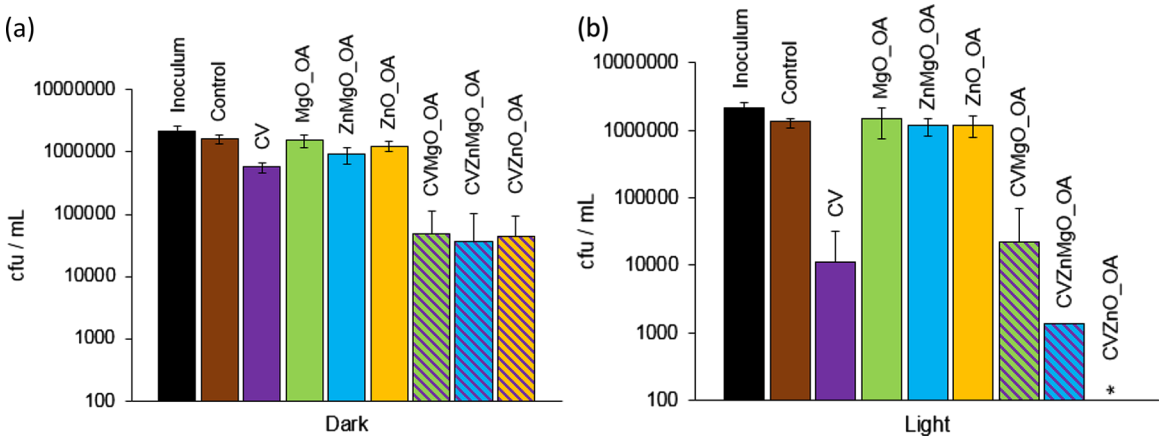

Figure 3. Viable counts of *S. aureus* 8325-4 after incubation at 20 °C on modified polyurethane squares for (a) 1 h in the dark and (b) 1 h with exposure to white-light illumination with an average light intensity of 6600 ± 900 lx at a distance of 25 cm from the samples. *Bacterial counts were reduced to below the detection limit of 100 cfu/mL. OA indicates NPs synthesized with OA capping. Error bars are based on the standard deviations of three experimental replicates.

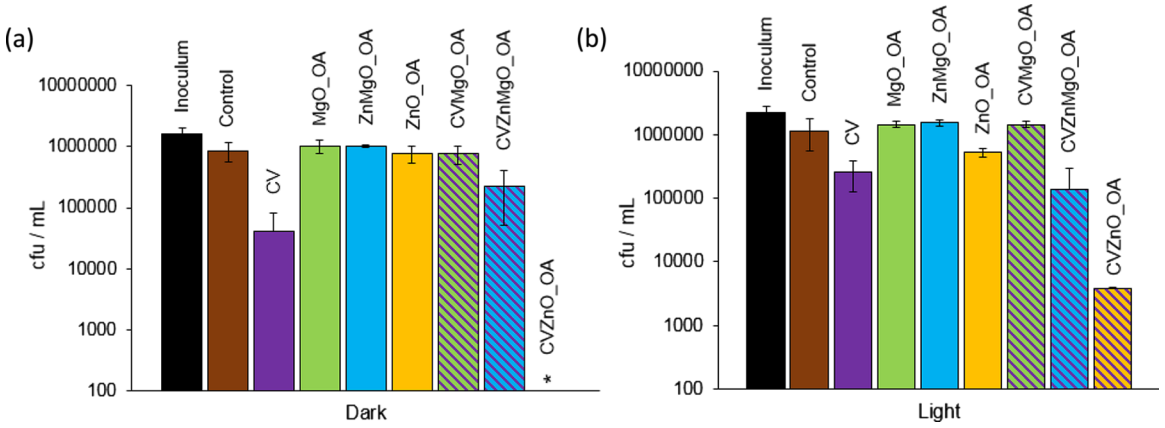

Figure 4. Viable counts of *E. coli* ATCC 25922 after incubation at 20 °C on modified polyurethane squares for (a) 4 h in the dark and (b) 2 h with exposure to white-light illumination with an average light intensity of 6600 ± 900 lx at a distance of 25 cm from the samples. *Bacterial counts were reduced to below the detection limit of 100 cfu/mL. OA indicates NPs synthesized with OA capping. Error bars are based on the standard deviation of three experimental replicates.

through the polymer matrix.[43] In this investigation, the NPs used were dispersed in different solvents: hexane for the oleate-capped NPs and toluene for the DOPA-capped NPs. Consequently, swelling measurements were conducted to ensure that in both cases the polymers swelled to the same extent. Immersion of the polymer samples in the DOPA-capped NP/toluene suspension for 24 h resulted in a 142% increase in the polymer size. In contrast to toluene, hexane is a poor solvent for polymer swelling and thus the oleate-capped NP swelling solution was optimized to a 1:1 ratio of hexane/DCM such that comparable swelling was achieved. This optimization should minimize differences in the concentrations of encapsulated NPs induced by polymer swelling. Additionally, a higher ratio of DCM compared to that of hexane (7.5:2.5) resulted in deformation of the polymer samples after swell-encapsulation; therefore, it was necessary to use a swelling solution that did not alter the appearance and properties of the sample for control purposes.

4.3. Microbiological Investigation. *4.3.1. Oleate-Capped NPs.* The antibacterial activity of the oleate-capped NP-encapsulated polyurethane samples was tested against *S. aureus* 8325-4[41,42] and *E. coli* ATCC 25922 as representative Gram-positive and Gram-negative bacteria, respectively (Figures 3 and 4), using a protocol described by Sehmi et al.[20] The bactericidal effects of the following polyurethane samples were tested: (1) control polymer, (2) CV-coated polymer (CV), (3) metal oxide NP-encapsulated polymers (MgO_OA, ZnMgO_OA, ZnO_OA), and (4) CV-coated and metal oxide NP-encapsulated polymers (CVMgO_OA, CVZnMgO_OA, CVZnO_OA). The samples were exposed to a white-light source, emitting an average light intensity of 6600 ± 900 lx at a distance of 25 cm from the samples, for up to 4 h. A further set of samples was tested in the dark for the same time periods. For completeness, the photobactericidal activity of the MgO_OA and ZnMgO_OA samples synthesized in this study are compared to that of ZnO_OA and CVZnO_OA previously described by Sehmi et al. (Figures 3 and 4).[20]

Figure 3a illustrates the bactericidal activity of all of the samples tested against *S. aureus* 8325-4 following 1 h of incubation in the dark. Only samples containing combinations of NPs and dye resulted in significant killing of *S. aureus* 8325-4 (~1.5 log; $P = 0.002$). However, after 1 h of white-light exposure (Figure 3b), CV and CVMgO_OA resulted in an ~2 log reduction in *S. aureus* 8325-4. CVZnMgO_OA and CVZnO_OA samples caused complete killing, with

DOI: 10.1021/acsomega.6b00017
ACS Omega 2016, 1, 334−343

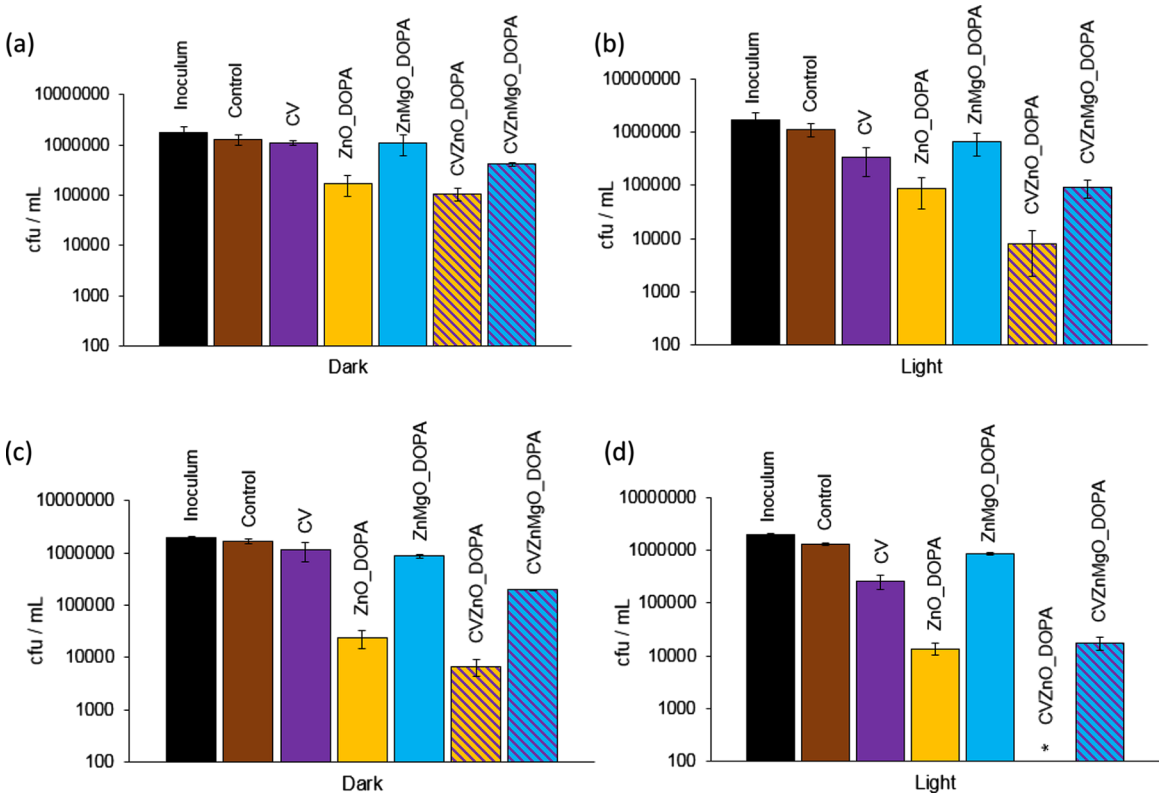

Figure 5. Viable counts of *E. coli* ATCC 25922 after incubation at 20 °C on modified polyurethane squares for (a) 2 h in the dark, (b) 2 h with exposure to standard laboratory white light (500 ± 300 lx), (c) 3 h in the dark, and (d) 3 h with exposure to standard laboratory white light (500 ± 300 lx). *Bacterial counts were reduced to below the detection limit of 100 cfu/mL. DOPA indicates NPs synthesized with DOPA capping. Error bars are based on the standard deviations of three experimental replicates.

CVZnO_OA reducing the bacterial numbers to below the detection limit (P = 0.002). Within 2 h of incubation, CVMgO_OA, CVZnMgO_OA, and CVZnO_OA samples all demonstrated highly significant bactericidal activity against *S. aureus* 8325-4 (≥4 log reduction; P = 0.002), under both white-light and dark conditions (Figure S11). Moreover, irradiated CV-coated samples also reduced *S. aureus* 8325-4 levels to below the detection limit within this time period.

These samples were subsequently tested against *E. coli* ATCC 25922 (Figure 4), and it was found that within 2 h the CV sample achieved an ∼0.5 log reduction in bacterial numbers under white-light activation. The presence of NPs enhanced this effect, with the CVZnMgO_OA sample resulting in a 1 log reduction in bacterial numbers and CVZnO_OA achieving a 2.5 log reduction (P = 0.002). Incubation in the dark for 4 h resulted in considerable activity against *E. coli* ATCC 25922, with bacterial numbers reduced to below the detection limit with the CVZnO_OA sample (Figure 4b). Note that 4 h of irradiation of all CV-incorporated samples resulted in potent photobactericidal activity (≥4 log; P = 0.002).

4.3.2. DOPA-Capped NPs. The bactericidal properties of the polyurethane samples encapsulated with DOPA-capped ZnO and ZnMgO NPs were also tested against *E. coli*. However, in this case the activities of the samples were enhanced using a low-intensity white-light source (500 ± 300 lx), comparable to the dim lighting in a hospital environment, which can range from 10 000 to 200 lx.[44] The polymer squares were exposed to ambient laboratory lighting conditions on a laboratory bench. To test the materials using conditions close to the real-world situation in other respects, the bacterial suspension in contact with the material was not covered with a coverslip and the samples were not placed in a humidity chamber. We have used coverslips previously to ensure close, uniform contact between the bacteria and the hydrophobic polymer surface, and a humidity chamber was used to prevent evaporation. It should be noted that in the absence of a coverslip there was no visible evidence that the bacterial suspension dried up over the course of the experiment.

The photobactericidal properties of the following polyurethane samples were tested: (1) control polymer, (2) CV-coated polymer (CV), (3) NP-encapsulated polymers (ZnMgO_DOPA, ZnO_DOPA), and (4) CV- and NP-encapsulated polymers (CVZnMgO_DOPA, CVZnO_DOPA). As the MgO_OA polyurethane sample did not effectively reduce bacterial numbers, DOPA-capped MgO NPs were not synthesized or tested for antibacterial activity. DOPA-capped ZnO NPs and DOPA-capped-ZnMgO NPs were much smaller in size than the corresponding oleate-capped NPs (2−4 nm compared to 15−18 nm).

In the dark (Figure 5a), no bactericidal activity was detected for the control sample, CV-coated polyurethane, and ZnMgO_DOPA-encapsulated polyurethane when incubated with *E. coli* ATCC 25922 for 2 h. However, within 3 h in the dark (Figure 5c), a significant reduction in bacterial numbers (∼2 log; P = 0.002) was noted for the ZnO_DOPA samples on their own, with an ∼0.5 log enhancement in bactericidal activity upon incorporation of CV (2.5 log, CVZnO_DOPA sample). The ZnMgO sample CVZnMgO_DOPA, however, showed a comparatively reduced activity, with an ∼1 log reduction in bacterial numbers (P = 0.002) in the dark. Irradiation of the CV

DOI: 10.1021/acsomega.6b00017
ACS Omega 2016, 1, 334−343

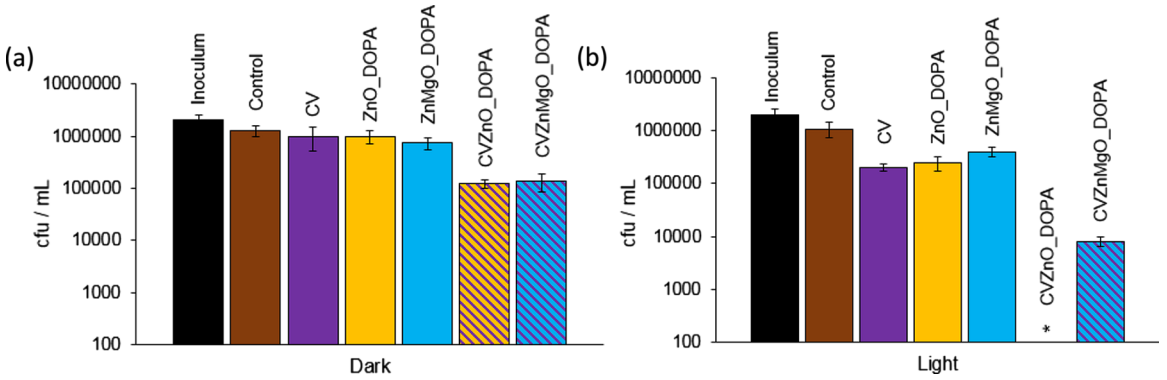

Figure 6. Viable counts of EMRSA-16 after incubation at 20 °C on modified polyurethane squares for (a) 2 h in the dark and (b) 2 h with exposure to standard laboratory white light (500 ± 300 lx). *Bacterial counts were reduced to below the detection limit of 100 cfu/mL. DOPA indicates NPs synthesized with DOPA capping. Error bars are based on the standard deviations of three experimental replicates.

samples using standard laboratory lighting for 2 h (Figure 5b) resulted in some photoactivated antibacterial activity (~0.7 log reduction), whereas the ZnO_DOPA samples showed similar antibacterial efficacies under light and dark conditions after 2 h (~2 log reduction). These findings suggest that the bactericidal mechanism of the ZnO_DOPA sample is via a non-photoactivated route, for example, absorption by the bacteria or coordination of the bacteria to the ZnO surface. The CVZnMgO_DOPA and CVZnO_DOPA samples induced lethal photosensitization of *E. coli* ATCC 25922; the former resulted in a 2 log reduction (P = 0.002), whereas the latter reduced the bacterial numbers to below the detection limit (≥4 log; P = 0.002) within 3 h of irradiation.

These samples incorporated with NPs and dye were also tested against an epidemic strain of MRSA (EMRSA-16; *S. aureus* NCTC 13143) using white-light irradiation (~500 lx). These samples were not placed in a humidity chamber, and no coverslip was used, to mimic the conditions of real-world exposure. In the dark, only the CVZnO_DOPA and CVZnMgO_DOPA samples demonstrated bactericidal activity against *S. aureus* NCTC 13143 (~1 log; P = 0.002; Figure 6a). The ZnMgO_DOPA, ZnO_DOPA, and CV samples showed limited photoactivated antimicrobial activities, reducing the numbers of *S. aureus* NCTC 13143 by 0.4 log, 0.6 log, and 0.8 log, respectively, within 2 h of white-light irradiation (500 lx; Figure 6b). However, the CV−NP combinations demonstrated enhanced photobactericidal activities: CVZnMgO_DOPA caused a 2 log reduction in the numbers of *S. aureus* NCTC 13143 (P = 0.002), whereas the CVZnO_DOPA sample was the most efficacious and reduced the bacterial numbers to below the detection limit (≥4 log; P = 0.002).

These results demonstrate the increased efficacy of ZnO NPs (both DOPA-capped and oleate-capped) when combined with CV, compared to that of MgO or ZnMgO. Note that two methods for Mg doping of ZnO were attempted, and neither achieved enhanced antibacterial activity compared to that of ZnO. Moreover, ZnO_DOPA-encapsulated polyurethane demonstrated the highest bactericidal activity against *E. coli* ever reported for ZnO-incorporated materials (with and without white-light activation) (Figure 4c,d). This may be attributed to the small size of ZnO_DOPA NPs (~2−4 nm) compared to that of ZnO_OA NPs (~18 nm). Previous studies have shown that smaller NPs are more effective at reducing the numbers of *E. coli*.[30] This is presumably accounted for by the easier penetration of small NPs through the cytoplasmic membrane of bacteria, enabling them to reach targets in the cytoplasm.[45,46]

4.3.3. Comparison between DOPA- and OA-Capped ZnMgO NPs. Additional experiments were carried out to evaluate the antibacterial activity of CVZnMgO_DOPA against *S. aureus* 8325-4 and *E. coli* ATCC 25922 at a range of light intensities and incubation periods (Table 1). Both the

Table 1. Summary of the Antibacterial Activity of CVZnMgO_DOPA against (a) *S. aureus* 8325-4 and (b) *E. coli* ATCC 25922[a]

time (h)	dark	500 ± 300 lx	6600 ± 900 lx
	(a) *S. aureus*		
6	1 log	≥4 log	≥4 log
4	1 log	3 log	≥4 log
2	0.5 log	1 log	≥4 log
1	no kill	no kill	3 log
	(b) *E. coli*		
6	1 log	≥4 log	≥4 log
4	0.5 log	3 log	≥4 log
2	no kill	1 log	2 log

[a]After various incubation times in the dark and on exposure to standard laboratory lighting (500 ± 300 lx) and a white-light source emitting 6600 ± 900 lx.

CVZnMgO_DOPA and CVZnMgO_OA samples achieved a 3 log reduction against *S. aureus* 8325-4 within 1 h of ~6600 lx white-light exposure. However, in the dark, within the same time period, CVZnMgO_DOPA does not demonstrate any significant antibacterial activity, whereas CVZnMgO_OA samples reduce the bacterial numbers by ~1.5 log. Moreover, on incubation for 2 h in the dark, the CVZnMgO_OA sample reduces the bacterial numbers to below the detection limit, compared to the CVZnMgO_DOPA sample, which only causes a 0.5 log reduction in *S. aureus* 8325-4 numbers (Figure S10).

Table 1b summarizes the performance of CVZnMgO samples when tested against *E. coli* ATCC 25922 under different lighting and incubation conditions. Both CVZnMgO_DOPA and CVZnMgO_OA demonstrate similar antibacterial efficacies in the dark within 4 h. This is unsurprising, as it has been previously noted that OA-capped NPs enhance bactericidal activity in the dark when tested against *E. coli* ATCC 25922.[47] However, distinct differences in the antibacterial performance were observed upon 2 h of white-light exposure, where the CVZnMgO_DOPA sample reduced

DOI: 10.1021/acsomega.6b00017
ACS Omega 2016, 1, 334−343

E. coli numbers twice as effectively as the CVZnMgO_OA sample.

These results suggest that the capping ligand plays a crucial role in the bactericidal activity against Gram-positive bacteria, such that CV samples containing oleate-capped ZnMgO NPs are more efficacious than those containing equivalent DOPA-capped NPs. This enhanced activity may be attributed to the bactericidal properties of the oleate ligand itself. Similar bactericidal activities in the dark were observed by Noimark et al. for TiO_2^-- and Au/TiO_2^--encapsulated silicone samples.[47] Here, the NPs were capped with OA, which has been observed to inhibit the growth of Gram-positive bacteria, such as *S. aureus*.[47] CVZnO_DOPA and ZnO_DOPA displayed greater antibacterial activity against *E. coli* and MRSA than CVZnMgO_DOPA and ZnMgO_DOPA under the light and dark conditions (Figure 5). However, the ZnO_DOPA and ZnMgO_DOPA samples displayed similar levels of Zn^{2+} leaching (Table S2), which indicates that leaching is not entirely responsible for the observed bactericidal activity in the dark. Additionally, ZnMgO_OA and ZnMgO_DOPA demonstrated similar levels of Zn^{2+} and Mg^{2+} leaching (Table S2), yet CVZnMgO_OA and CVZnMgO_DOPA exhibited different bactericidal activities against *S. aureus* 8325-4 after 1 h (~1.5 log reduction and no reduction in bacteria, respectively). Thus, the minimal amounts of leaching that occur from the modified polymer samples are not responsible for their antibacterial activities.

MgO-incorporated polyurethane exhibited poor activity against both bacteria. However, CVMgO-incorporated samples were effective against *S. aureus* 8325-4. This provides further evidence to suggest that the OA-capped agent is able to kill *S. aureus* 8325-4 when combined with CV, as no bactericidal activity was observed against *E. coli* ATCC 25922 on using CVMgO_OA under light or dark conditions within 2 h (Figure S12). We have shown that the addition of Mg as a dopant to ZnO NPs is detrimental to their antibacterial activity; further studies are underway to probe the surface and electronic properties of ZnMgO_DOPA NPs to attempt to understand the effect of this added Mg.

Polyurethane encapsulated with DOPA-capped NPs was tested against an epidemic strain of MRSA (EMRSA-16; *S. aureus* NCTC 13143) that is rife in hospitals throughout the United Kingdom.[41,42,48] To mimic more closely the conditions of natural exposure of the bacteria to the material, the experiment was carried out without using a coverslip or a humidity chamber. The CVZnO_DOPA sample induced lethal photosensitization of *S. aureus* NCTC 13143, resulting in a ≥4 log reduction in the bacterial numbers, whereas CVZnMgO_-DOPA achieved an ~2.5 log reduction within 2 h of irradiation.

This article presents a detailed study on the effects of the presence of CV, NP size, NP-capping ligand, Mg doping, and light intensity conditions on the antibacterial activity of polyurethane. Doping of ZnO with Mg did not result in an enhancement of the antibacterial activity under either light or dark conditions when the samples were tested against both Gram-positive and Gram-negative bacteria. In line with the previous literature,[30,31,49−51] the greatest bactericidal activity was exhibited when smaller NPs were used. However, when the NPs were incorporated with CV, the antibacterial activity of the samples could be further enhanced by tuning the NP capping group. Modification of the NP surfaces with different capping agents can alter their toxicities, causing differences between ROS generation and Zn^{2+} release.

The possible mechanisms for the antibacterial activity of ZnO NPs include ROS formation and oxidative stress,[20] Zn^{2+} release,[30] electrostatic interaction,[23,30] and internalization of the NPs into the bacteria.[23] Bacterial cell walls have an overall negative charge, which facilitates electrostatic interactions between the bacteria and CV and Zn^{2+} on the surface of the polymer, assisting in bacterial killing. In this study, differences in the antibacterial activities of ZnO-incorporated samples were apparent between Gram-positive and Gram-negative bacteria, presumably as a result of differences in the cell-wall structures: Gram-positive bacteria have a thick peptidoglycan layer (20−80 nm), whereas Gram-negative bacteria have a thinner layer of peptidoglycan (7−8 nm) and a second outer membrane.[52] In keeping with previous studies,[18−22,42,51] Gram-negative bacteria were found to be less susceptible to dye- and NP-incorporated polymeric surfaces. This may be due to the reduced penetration of radicals through the double cell membrane of Gram-negative bacteria. Further studies will focus on testing the antibacterial activities of these surfaces against more strains to understand the differences between bacterial reduction of Gram-positive and Gram-negative bacteria. It is possible that the smaller NPs are able to penetrate through the bacterial cell wall more effectively than the larger 15−18 nm NPs. The fact that polyurethane containing ZnO_DOPA, which is only 3 nm in size, shows antibacterial activity under light and dark conditions without CV (Figures 5 and 6) supports this argument. The killing by ZnO_DOPA observed in the dark also suggests that nonphotoactivated bactericidal activity occurs, either because NPs penetrate into the bacterial cells or because they produce ROS by interacting with defects on the polymer surface. Further tests were performed to examine whether the amount of ZnO NP leaching (shown in Table S2) was sufficient to reduce the bactericidal activity of ZnO_DOPA. The samples were immersed in water for 48 h and then removed and tested against *E. coli* ATCC 25922. The antibacterial activity of ZnO_DOPA did not differ under the light or dark condition after immersion in water (data not shown), which indicates that leaching of the ZnO NPs is not sufficient to reduce the bactericidal activity of the polymer. Zinc leaching is shown to tail off over time, as all "loose" Zn is lost, which is also shown by Noimark et al.[22]

Typically, ZnO NPs have a wide band gap (3.53 eV for DOPA-capped ZnO),[22] requiring UV illumination for ROS generation. However, because of the presence of pre-existing surface defects on the NPs, gap states can produce ROS under lower-energy-light illumination[50] (i.e., visible light) and even in the dark. Moreover, samples with combinations of NPs and CV showed increased bactericidal activity in the dark. This may be due to defects on the NP surface, in addition to the intrinsic bactericidal properties of the dye itself. Previous studies have shown that the incorporation of a combination of ZnO and CV into polyurethane can enhance the antibacterial activity of the dye via both type I and type II mechanistic pathways.[20] It is anticipated that these bactericidal surfaces will produce photogenerated species that can oxidize organic contaminants on the surface so that they maintain their bactericidal properties. Additionally, bacterial resistance is unlikely to occur as these surfaces operate via multiple attack mechanisms. These polymers have demonstrated considerable antibacterial activity against a higher bacterial load than that likely to occur in a clinical setting: $\sim 1 \times 10^5$ cfu/cm^{-2} of bacteria used in this investigation compared to $\sim 1 \times 10^2$ cfu/cm^{-2} found in hospitals.[22,53,54]

DOI: 10.1021/acsomega.6b00017
ACS Omega 2016, 1, 334−343

5. CONCLUSIONS

For the first time, polymers containing NPs and dye were tested against an epidemic isolate of MRSA (EMRSA-16; *S. aureus* NCTC 13143) under laboratory lighting conditions (~13× less intense than the lighting conditions in previous studies performed by our group). These experiments were conducted on the bench, with no barrier (coverslip) between the inoculum and the environment, to determine the efficacy of these antimicrobial polymers under conditions similar to those found naturally. Oleate-capped NPs combined with CV are biocompatible and highly effective at reducing the numbers of Gram-positive bacteria, possibly due to the antibacterial properties of the oleate ligand itself. ZnO_DOPA (2−4 nm) was able to reduce the numbers of *E. coli* without a need for a photosensitizer or white-light activation. We observed highly significant bactericidal activity by CVZnO_DOPA against an epidemic strain of MRSA. This study established polyurethane incorporated with CV and ZnO or ZnMgO NPs as a highly effective antibacterial surface, under conditions that mimic natural exposure in clinical environments. This technology shows promise for use in hospitals to reduce bacterial surface contamination and, ultimately, the risk for HCAIs.

■ ASSOCIATED CONTENT

Supporting Information

The Supporting Information is available free of charge on the ACS Publications website at DOI: 10.1021/acsomega.6b00017.

Materials characterization, energy-dispersive X-ray, UV−vis absorbance spectroscopy, X-ray diffraction, XPS, water contact angle measurements, photostability of polymers, additional microbiology, and leaching study results (PDF)

■ AUTHOR INFORMATION

Corresponding Author

*E-mail: a.macrobert@ucl.ac.uk.

Notes

The authors declare no competing financial interest.

■ ACKNOWLEDGMENTS

S.S. would like to thank Dr. S. Sathasivam for his help with XPS and for the award of an Impact studentship from UCL. The EPSRC is acknowledged for research funding by ICL (EP/K035274/1 and EP/M013839/1) and by UCL (EP/M015157/1 and EP/M506448/1).

■ REFERENCES

(1) Sydnor, E. R. M. Healthcare-associated infections fact sheet, World Health Organization: Patient Safety, 2012, http://www.who.int/gpsc/country_work/gpsc_ccisc_fact_sheet_en.pdf (accessed Jun 28, 2016).

(2) Sydnor, E. R. M.; Perl, T. M. Hospital Epidemiology and Infection Control in Acute-Care Settings. *Clin. Microbiol. Rev.* **2011**, *24*, 141−173.

(3) Review of Scientific Data Regarding Transmission of Infectious Agents in Healthcare Settings, Centers for Disease Control and Prevention, 2007, http://www.cdc.gov/hicpac/pdf/isolation/Pages12_40_Isolation2007.pdf (accessed Jun 28, 2016).

(4) World Health Organization Guidelines on Hand Hygiene in Health Care: a Summary, 2009, http://apps.who.int/iris/bitstream/10665/70126/1/WHO_IER_PSP_2009.07_eng.pdf (accessed Jun 28, 2016).

(5) Page, K.; Wilson, M.; Parkin, I. P. Antimicrobial surfaces and their potential in reducing the role of the inanimate environment in the incidence of hospital-acquired infections. *J. Mater. Chem.* **2009**, *19*, 3819−3831.

(6) Goodman, S. B.; Yao, Z.; Keeney, M.; Yang, F. The future of biologic coatings for orthopaedic implants. *Biomaterials* **2013**, *34*, 3174−3183.

(7) Noimark, S.; Dunnill, C. W.; Wilson, M.; Parkin, I. P. The role of surfaces in catheter-associated infections. *Chem. Soc. Rev.* **2009**, *38*, 3435−3448.

(8) Noimark, S.; Dunnill, C. W.; Kay, C. W. M.; Perni, S.; Prokopovich, P.; Ismail, S.; Wilson, M.; Parkin, I. P. Incorporation of methylene blue and nanogold into polyvinyl chloride catheters; a new approach for light-activated disinfection of surfaces. *J. Mater. Chem.* **2012**, *22*, 15388.

(9) Bovis, M. J.; Noimark, S.; Woodhams, J. H.; Kay, C. W. M.; Weiner, J.; Peveler, W. J.; Correia, A.; Wilson, M.; Allan, E.; Parkin, I. P.; MacRobert, A. J. Photosensitisation studies of silicone polymer doped with methylene blue and nanogold for antimicrobial applications. *RSC Adv.* **2015**, *5*, 54830.

(10) Shrestha, A.; Hamblin, M. R.; Kishen, A. Photoactivated rose bengal functionalized chitosan nanoparticles produce antibacterial/biofilm activity and stabilize dentin-collagen. *Nanomedicine* **2014**, *10*, 491−501.

(11) Kim, Y. S.; Park, S. J.; Lee, E. J.; Cerbo, R. M.; Lee, S. M.; Ryu, C. H.; Kim, G. S.; Kim, J. O.; Ha, Y. L. Antibacterial compounds from Rose Bengal-sensitized photooxidation of beta-caryophyllene. *J. Food Sci.* **2008**, *73*, C540−C545.

(12) Piccirillo, C.; Perni, S.; Gil-Thomas, J.; Prokopovich, P.; Wilson, M.; Pratten, J.; Parkin, I. P. Antimicrobial activity of methylene blue and toluidine blue O covalently bound to a modified silicone polymer surface. *J. Mater. Chem.* **2009**, *19*, 6167−6171.

(13) Sauer, K.; Steczko, J. S. R. Ash, Effect of a solution containing citrate/Methylene Blue/parabens on *Staphylococcus aureus* bacteria and biofilm, and comparison with various heparin solutions. *J. Antimicrob. Chemother.* **2009**, *63*, 937−945.

(14) Wainwright, M.; Phoenix, D. A.; Gaskell, M.; Marshall, B. Photobactericidal activity of methylene blue derivatives against vancomycin-resistant Enterococcus spp. *J. Antimicrob. Chemother.* **1999**, *44*, 823−825.

(15) Perni, S.; Piccirillo, C.; Kafizas, A.; Uppal, M.; Pratten, J.; Wilson, M.; Parkin, I. P. Antibacterial Activity of Light-Activated Silicone Containing Methylene Blue and Gold Nanoparticles of Different Sizes. *J. Clust. Sci.* **2010**, *21*, 427−438.

(16) Choi, S. S.; Lee, H. K.; Chae, H. S. In vitro photodynamic antimicrobial activity of methylene blue and endoscopic white light against Helicobacter pylori 26695. *J. Photochem. Photobiol., B* **2010**, *101*, 206−209.

(17) Adams, E. The antibacterial action of Crystal Violet. *J. Pharm. Pharmacol.* **1967**, *19*, 821−826.

(18) Ozkan, E.; Allan, E.; Parkin, I. P. The antibacterial properties of light-activated polydimethylsiloxane containing crystal violet. *RSC Adv.* **2014**, *4*, 51711.

(19) Hwang, G. B.; Allan, E.; Parkin, I. P. White light-activated antimicrobial paint using crystal violet. *ACS Appl. Mater. Inter.* **2016**, *8*, 15033−15039.

(20) Sehmi, S.; Noimark, S.; Bear, J. C.; Peveler, W. J.; Bovis, M.; Allan, E.; MacRobert, A. J.; Parkin, I. P. Lethal photosensitisation of *Staphylococcus aureus* and *Escherichia coli* using crystal violet and zinc oxide-encapsulated polyurethane. *J. Mater. Chem. B.* **2015**, *3*, 6490.

(21) Noimark, S.; Bovis, M.; MacRobert, A. J.; Correia, A.; Allan, E.; Wilson, M.; Parkin, I. P. Photobactericidal polymers; the incorporation of crystal violet and nanogold into medical grade silicone. *RSC Adv.* **2013**, *3*, 18383.

(22) Noimark, S.; Weiner, J.; Noor, N.; Allan, E.; Williams, C. K.; Shaffer, M. S. P.; Parkin, I. P. Antimicrobial Surfaces: Dual-Mechanism Antimicrobial Polymer−ZnO Nanoparticle and Crystal Violet-Encapsulated Silicone. *Adv. Funct. Mater.* **2015**, *25*, 1367−1373.

DOI: 10.1021/acsomega.6b00017
ACS Omega 2016, 1, 334−343

(23) Lakshmi Prasanna, V.; Vijayaraghavan, R. Insight into the Mechanism of Antibacterial Activity of ZnO: Surface Defects Mediated Reactive Oxygen Species Even in the Dark. *Langmuir* **2015**, *31*, 9155−9162.
(24) Li, Y.; Zhang, W.; Niu, J.; Chen, Y. Mechanism of photogenerated reactive oxygen species and correlation with the antibacterial properties of engineered metal-oxide nanoparticles. *ACS Nano.* **2012**, *6*, 5164−5173.
(25) Leung, Y. H.; Ng, A. M. C.; Xu, X.; Shen, Z.; Gethings, L. A.; Wong, M. T.; Chan, C. M. N.; Guo, M. Y.; Ng, Y. H.; Djurisic, A. B.; Lee, P. K. H.; Chan, W. K.; Yu, L. H.; Phillips, D. L.; Ma, A. P. Y.; Leung, F. C. C. Mechanisms of antibacterial activity of MgO: non-ROS mediated toxicity of MgO nanoparticles towards *Escherichia coli*. *Small* **2014**, *10*, 1171−1183.
(26) Tang, Z.; Lv, B. MgO nanoparticles as antibacterial agent: preparation and activity. *Braz. J. Chem. Eng.* **2014**, *31*, 591−601.
(27) Sawai, J. Quantitative evaluation of antibacterial activities of metallic oxide powders (ZnO, MgO and CaO) by conductimetric assay. *J. Microbiol. Methods* **2003**, *54*, 177−182.
(28) Sundrarajan, M.; Suresh, J.; Gandhi, R. R. A comparative study on antibacterial properties of MgO nanoparticles prepared under different calcination temperature. *Digest J. Nanomater. Biostruct.* **2012**, *7*, 983−989.
(29) Jin, T.; He, Y. Antibacterial activities of magnesium oxide (MgO) nanoparticles against foodbourne pathogens. *J. Nanopart. Res.* **2011**, *13*, 6877−6885.
(30) Sirelkhatim, A.; Mahmud, S.; Seeni, A.; Kaus, N. H. M.; Ann, L. C.; Bakhori, S. K. M.; Hasan, H.; Mohamad, D. Review on Zinc Oxide Nanoparticles. *Nano-Micro Lett.* **2015**, *7*, 219−242.
(31) Seil, J. T.; Webster, T. J. Antimicrobial applications of nanotechnology: methods and literature. *Int. J. Nanomed.* **2012**, *7*, 2767−2781.
(32) Guo, B.; Guo, L.; Cao, Y.; Li, A.; Kong, J.; Zhai, H.; Wu, D. The antibacterial activity of Ta-doped ZnO nanoparticles. *Nanoscale Res. Lett.* **2015**, *10*, No. 1047, DOI: 10.1186/s11671-015-1047-4.
(33) Nair, M. G.; Nirmala, M.; Rekha, K.; Anukaliani, A. Structural, optical, photocatalytic and antibacterial activity of ZnO and Co doped ZnO nanoparticles. *Mater. Lett.* **2011**, *65*, 1797−1800.
(34) Rekha, K.; Nirmala, M.; Nair, M. G.; Anukaliani, A. Structural, optical, photocatalytic and antibacterial activity of zinc oxide and manganese doped zinc oxide nanoparticles. *Phys. B* **2010**, *405*, 3180−3185.
(35) Jan, T.; Iqbal, J.; Ismail, M.; Zakaullah, M.; Naqvi, S. H.; Badshah, N. Sn doping induced enhancement in the activity of ZnO nanostructures against antibiotic resistant *S. aureus* bacteria. *Int. J. Nanomed.* **2013**, *8*, 3679−3687.
(36) Sharma, N.; Jandaik, S.; Kumar, S.; Chitkara, M.; Sandhu, I. S. Synthesis, characterisation and antimicrobial activity of manganese- and iron-doped zinc oxide nanoparticles. *J. Exp. Nanosci.* **2016**, *11*, 54−71.
(37) Wang, B.; Callahan, M. J.; Bouthillette, L. O. Hydrothermal growth and photoluminescence of ZnMgO alloy crystals. *Cryst. Growth Des.* **2006**, *6*, 1256−1260.
(38) Etacheri, V.; Roshan, R.; Kumar, V. Mg-doped ZnO nanoparticles for efficient sunlight-driven photocatalysis. *ACS Appl. Mater. Interfaces* **2012**, *4*, 2717−2725.
(39) Park, J.; An, K.; Hwang, Y.; Park, J.; Noh, H.; Kim, J.; Park, J.; Hwang, N.; Hyeon, T. Ultra-large-scale syntheses of monodisperse nanocrystals. *Nat. Mater.* **2004**, *3*, 891−895.
(40) Brown, N. J.; Weiner, J.; Hellgardt, K.; Shaffer, M. S. P.; Williams, C. K. Phosphinate stabilised ZnO and Cu colloidal nanocatalysts for CO_2 hydrogenation to methanol. *Chem. Commun.* **2013**, *49*, 11074−11076.
(41) Herbert, S.; Ziebandt, A. K.; Ohlsen, K.; Schafer, T.; Hecker, M.; Albrecht, D.; Novick, R.; Gotz, F. Repair of global regulators in *Staphylococcus aureus* 8325 and comparative analysis with other clinical isolates. *Infect. Immun.* **2010**, *78*, 2877−2889.
(42) Das, S.; Anderson, C. J.; Grayes, A.; Mendoza, K.; Harazin, M.; Schora, D. M.; Peterson, L. R. Nasal Carriage of Epidemic Methicillin-Resistant *Staphylococcus aureus* 15 (EMRSA-15) Clone Observed in Three Chicago-Area Long-Term Care Facilities. *Antimicrob. Agents. Chemother.* **2013**, *57*, 4551−4553.
(43) Crick, C. R.; Noimark, S.; Peveler, W. J.; Bear, J. C.; Ivanov, A. P.; Edel, J. B.; Parkin, I. P. Advanced analysis of nanoparticle composites − a means towards increasing the efficiency of functional materials. *RSC Adv.* **2015**, *5*, 53789.
(44) Sehmi, S. K.; Noimark, S.; Weiner, J.; Allan, E.; MacRobert, A. J.; Parkin, I. P. Potent antibacterial activity of copper embedded into silicone and polyurethane. *ACS Appl. Mater. Interfaces* **2015**, *7*, 22807−22813.
(45) Verma, A.; Stellacci, F. Effect of surface properties on nanoparticle-cell interactions. *Small* **2010**, *6*, 12−21.
(46) De Jong, W. H.; Borm, P. J. Drug delivery and nanoparticles: Applications and hazards. *Int. J. Nanomed.* **2008**, *3*, 133−149.
(47) Noimark, S.; Page, K.; Bear, J. C.; Sotelo-Vazquez, C.; Quesada-Cabrera, R.; Lu, Y.; Allan, E.; Darr, J. A.; Parkin, I. P. Functionalised gold and titania nanoparticles and surfaces for use as antimicrobial coatings. *Faraday Discuss.* **2014**, *175*, 273.
(48) Johnson, A. P.; Aucken, H. M.; Cavendish, S.; Ganner, M.; Wale, M. C. J.; Warner, M.; Livermore, D. M.; Cookson, B. D. Dominance of EMRSA-15 and -16 among MRSA causing nosocomial bacteraemia in the UK: analysis of isolates from the European Antimicrobial Resistance Surveillance System (EARSS). *J. Antimicrob. Chemother.* **2001**, *48*, 143−144.
(49) Liu, H. L.; Dai, T. S. A.; Fu, K. Y.; Hsu, S. H. Antibacterial properties of silver nanoparticles in three different sizes and their nanocomposites with a new waterbourne polyurethane. *Int. J. Nanomed.* **2010**, *19*, 1017−1028.
(50) Jones, N.; Ray, B.; Koodali, R. T.; Adhar, M. C. Antibacterial activity of ZnO nanoparticles suspensions on a broad spectrum of microorganisms. *FEMS Microbiol. Lett.* **2008**, *279*, 71−76.
(51) Azam, A.; Ahmed, A. S.; Oves, M.; Khan, M. S.; Habib, S. S.; Memic, A. Antimicrobial activity of metal oxide nanoparticles against Gram-positive and Gram-negative bacteria: a comparative study. *Int. J. Nanomed.* **2012**, *7*, 6003−6009.
(52) Ponja, S. D.; Sehmi, S. K.; Allan, E.; MacRobert, A. J.; Parkin, I. P.; Carmalt, C. J. Enhanced bactericidal activity of silver thin films deposited via aerosol-assisted chemical vapour deposition. *ACS Appl. Mater. Interfaces* **2015**, *7*, 28616−28623.
(53) Noimark, S.; Allan, E.; Parkin, I. P. Light-activated antimicrobial surfaces with enhanced efficacy induced by a dark-activated mechanism. *Chem. Sci.* **2014**, *5*, 2216−2223.
(54) Ozkan, E.; Ozkan, F. T.; Allan, E.; Parkin, I. P. The use of zinc oxide nanoparticles to enhance the antibacterial properties of light-activated polydimethylsiloxane containing crystal violet. *RSC Adv.* **2015**, *5*, 8806−8813.

DOI: 10.1021/acsomega.6b00017
ACS Omega 2016, 1, 334−343